Electronic Supplementary Material (ESI) for Journal of Materials Chemistry A.

Electronic Supplementary Information (ESI)

Lewis Basic Sites (LBSs) functionalized zeolite-like supramolecular assemblies (ZSAs) with high performance of CO_2 sorption and highly selective CO_2/CH_4 separation

Jiantang Li, Cong Dai, Yu Cao, Xiaodong Sun, Guanghua Li, Qisheng Huo and Yunling Liu*

State Key Laboratory of Inorganic Synthesis and Preparative Chemistry, College of Chemistry, Jilin University, Changchun 130012, P. R. China.
**E-mail: yunling@jlu.edu.cn; Fax: +86-431-85168624; Tel: +86-431-85168614*

S1. Calculation procedures of selectivity from IAST

The measured experimental data is excess loadings (q^{ex}) of the pure components CO_2, CH_4, C_2H_6 and C_3H_8 for **ZSA-7**, **ZSA-8** and **ZSA-9**, which should be converted to absolute loadings (q) firstly.

$$q = q^{ex} + \frac{pVpore}{ZRT}$$

Here Z is the compressibility factor. The Peng-Robinson equation was used to estimate the value of compressibility factor to obtain the absolute loading, while the measure pore volume is also necessary.

The dual-site Langmuir-Freundlich equation is used for fitting the isotherm data at 298 K.

$$q = q_{m_1} \times \frac{b_1 \times p^{1/n_1}}{1 + b_1 \times p^{1/n_1}} + q_{m_2} \times \frac{b_2 \times p^{1/n_2}}{1 + b_2 \times p^{1/n_2}}$$

Here p is the pressure of the bulk gas at equilibrium with the adsorbed phase (kPa), q is the adsorbed amount per mass of adsorbent (mol/kg), q_{m1} and q_{m2} are the saturation capacities of sites 1 and 2 (mol/kg), b_1 and b_2 are the affinity coefficients of sites 1 and 2 (1/kPa), n_1 and n_2 are the deviations from an ideal homogeneous surface.

The selectivity of preferential adsorption of component 1 over component 2 in a mixture containing 1 and 2, perhaps in the presence of other components too, can be formally defined as

$$S = \frac{q_1/q_2}{p_1/p_2}$$

q_1 and q_2 are the absolute component loadings of the adsorbed phase in the mixture. These component loadings are also termed the uptake capacities. We calculate the values of q_1 and q_2 using the Ideal Adsorbed Solution Theory (IAST) of Myers and Prausnitz.

S2. Supporting Figures

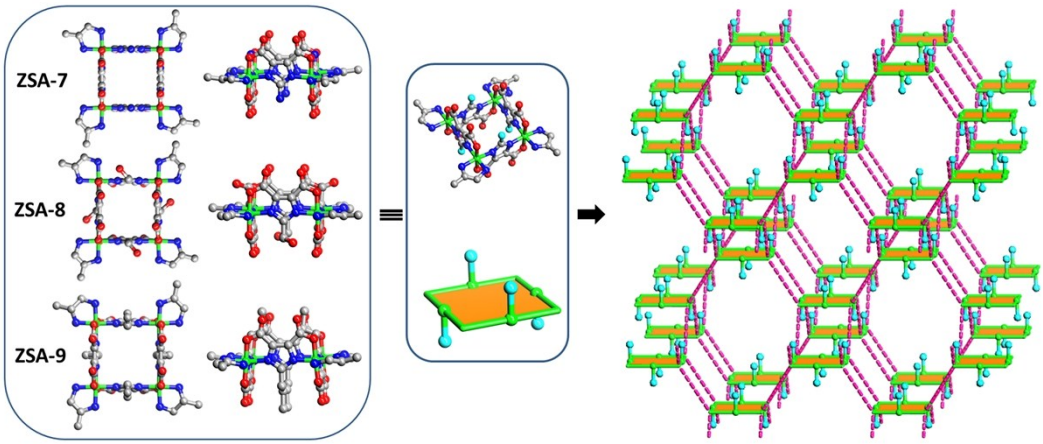

Fig. S1. Ball-and-stick and schematic representations of the substituents' orientation.

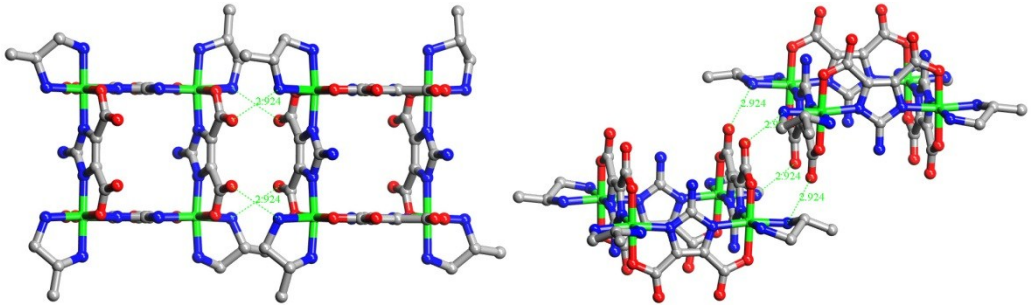

Fig. S2. Different direction views of four intermolecular N-H···O hydrogen bonds (2.924 Å) linking the vertices of two neighboring squares in **ZSA-7**.

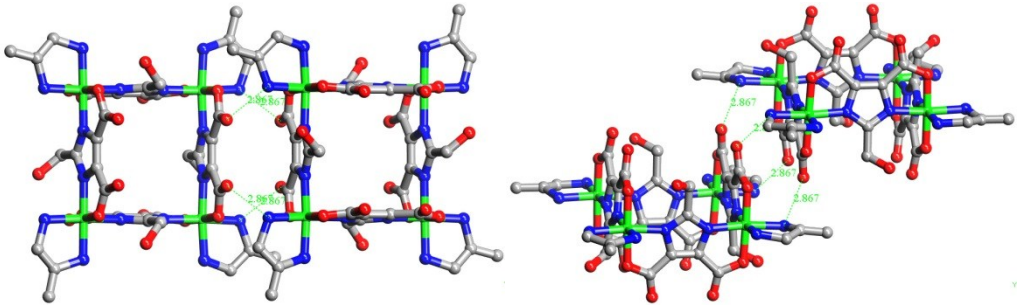

Fig. S3. Different direction views of four intermolecular N-H···O hydrogen bonds (2.867 Å) linking the vertices of two neighboring squares in **ZSA-8**.

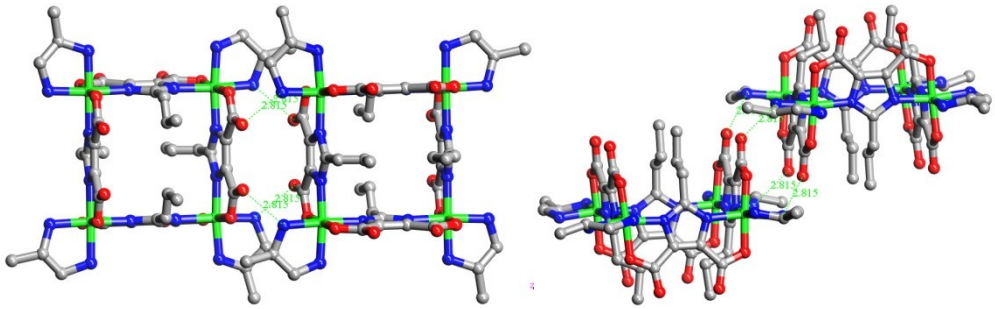

Fig. S4. Different direction views of four intermolecular N-H···O hydrogen bonds (2.815 Å) linking the vertices of two neighboring squares in **ZSA-9**.

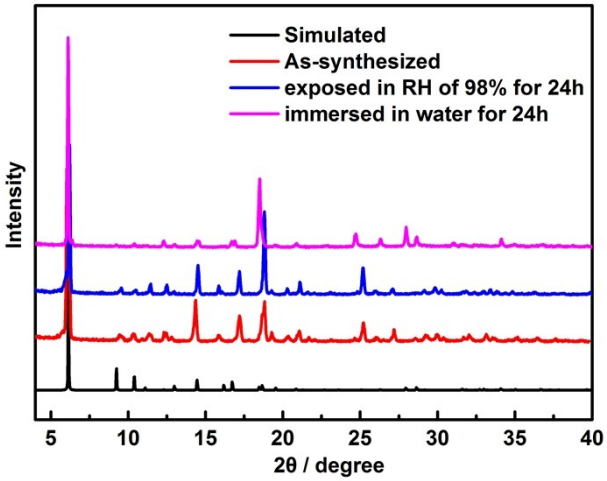

Fig. S5. PXRD patterns of **ZSA-7** for simulated, experimental samples, exposed in RH of 98% and immersed in water. The differences in reflection intensity are probably due to preferred orientations in the powder sample.

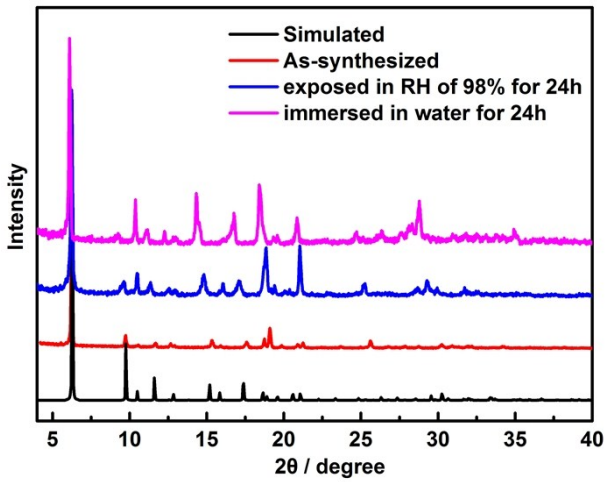

Fig. S6. PXRD patterns of **ZSA-8** for simulated, experimental samples, exposed in RH of 98% and immersed in water. The differences in reflection intensity are probably due to preferred orientations in the powder sample.

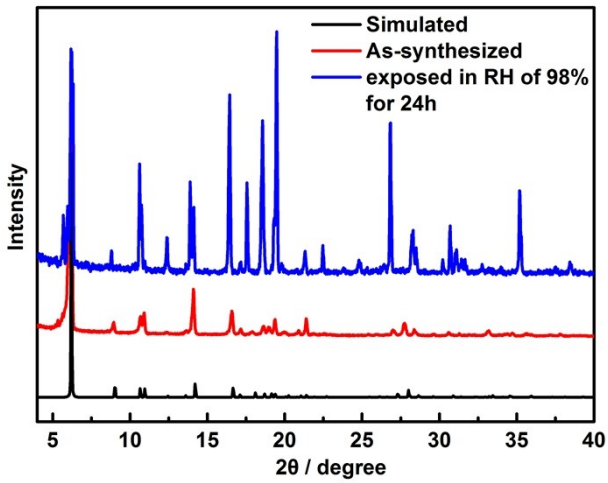

Fig. S7. PXRD patterns of **ZSA-9** for simulated, experimental samples and exposed in RH of 98%. The differences in reflection intensity are probably due to preferred orientations in the powder sample.

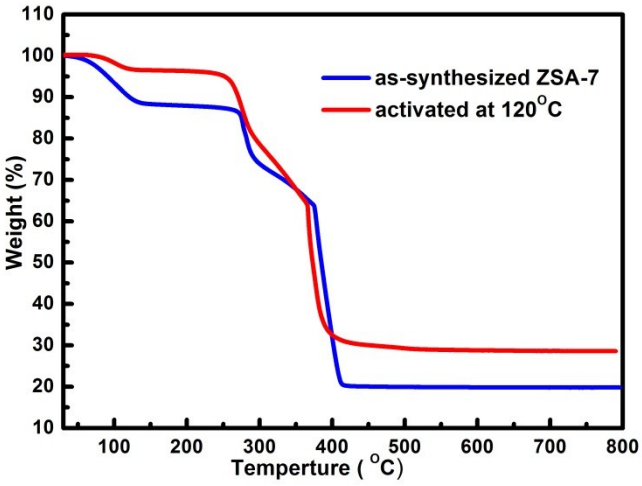

Fig. S8. Thermogravimetric analysis curves of **ZSA-7** for the as-synthesized and activated samples.

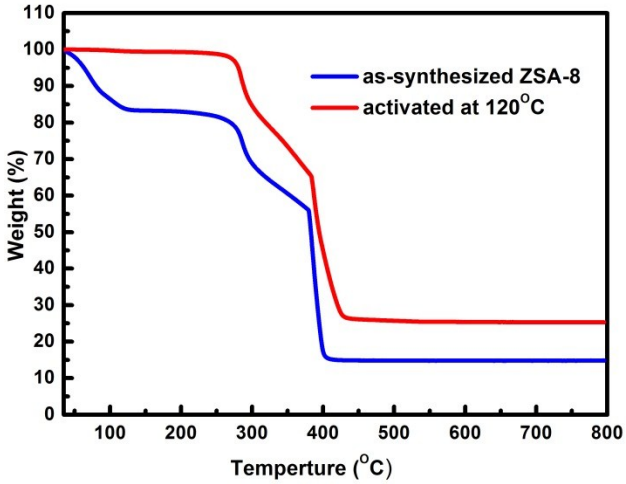

Fig. S9. Thermogravimetric analysis curves of **ZSA-8** for the as-synthesized and activated samples.

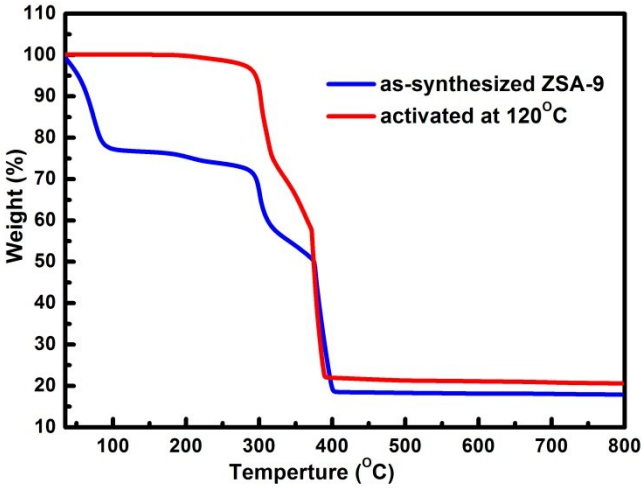

Fig. S10. Thermogravimetric analysis curves of **ZSA-9** for the as-synthesized and activated samples.

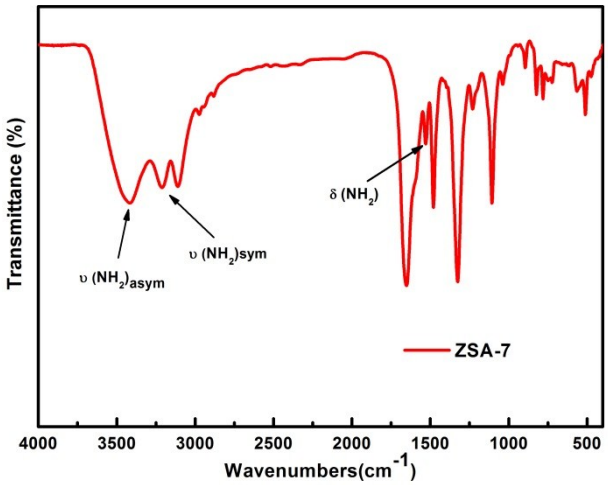

Fig. S11. FT-IR spectrum of **ZSA-7.**

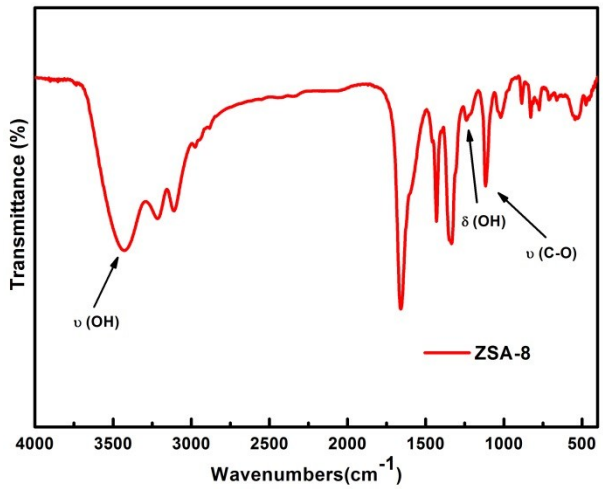

Fig. S12. FT-IR spectrum of **ZSA-8.**

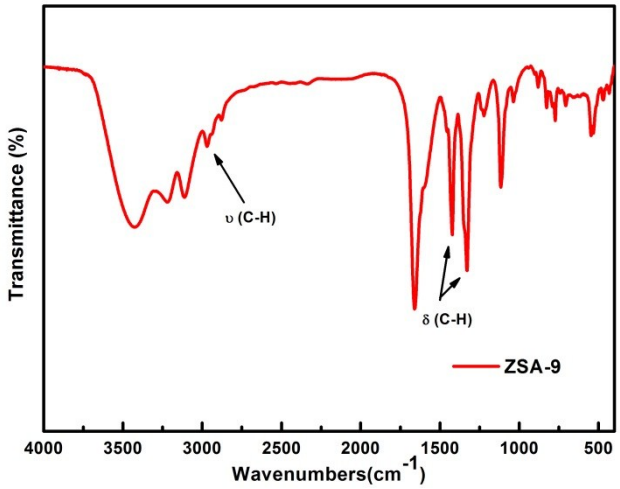

Fig. S13. FT-IR spectrum of **ZSA-9.**

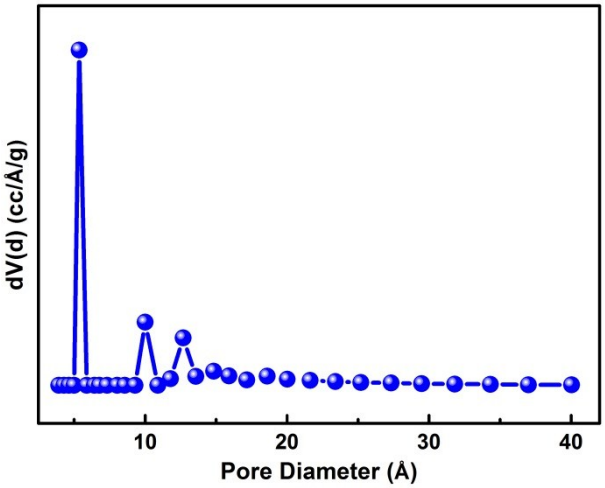

Fig. S14. The pore size distribution of **ZSA-7** calculated using the DFT method.

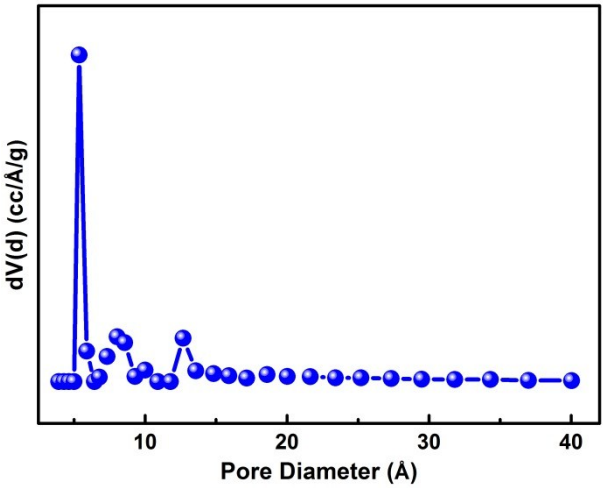

Fig. S15. The pore size distribution of **ZSA-8** calculated using the DFT method.

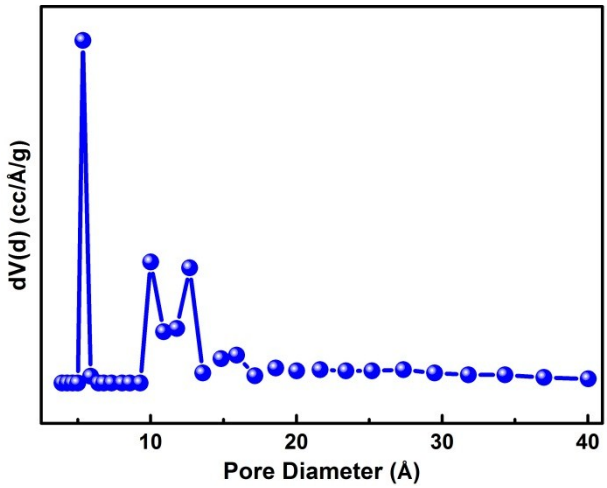

Fig. S16. The pore size distribution of **ZSA-9** calculated using the DFT method.

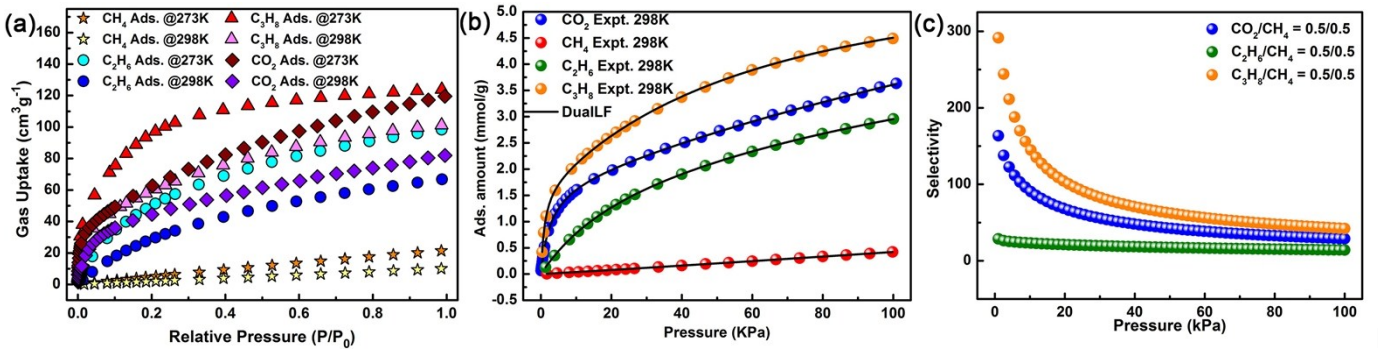

F

ig. S17. (a) Gas sorption isotherms for **ZSA-1**; (b) gas sorption isotherms of CO_2, CH_4, C_2H_6 and C_3H_8 along with the dual-site Langmuir−Freundlich (DSLF) fits for **ZSA-1**; (c) gas mixture adsorption selectivities for **ZSA-1** predicted by IAST at 298 K under 1 bar.

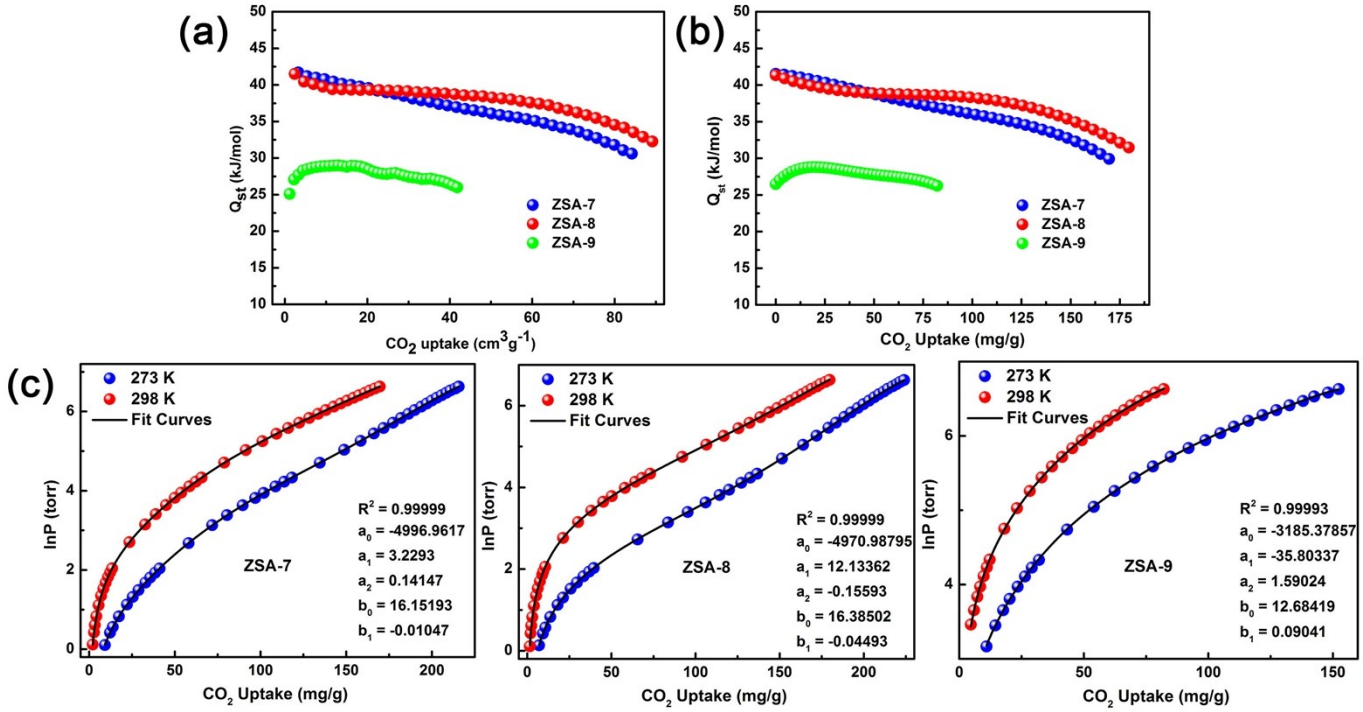

Fig. S18. Q_{st} of CO_2 for **ZSA-7**, **ZSA-8** and **ZSA-9**. (a) calculated by MicroActive soft; (b) calculated with virial method; (c) nonlinear curves fitting of CO_2.

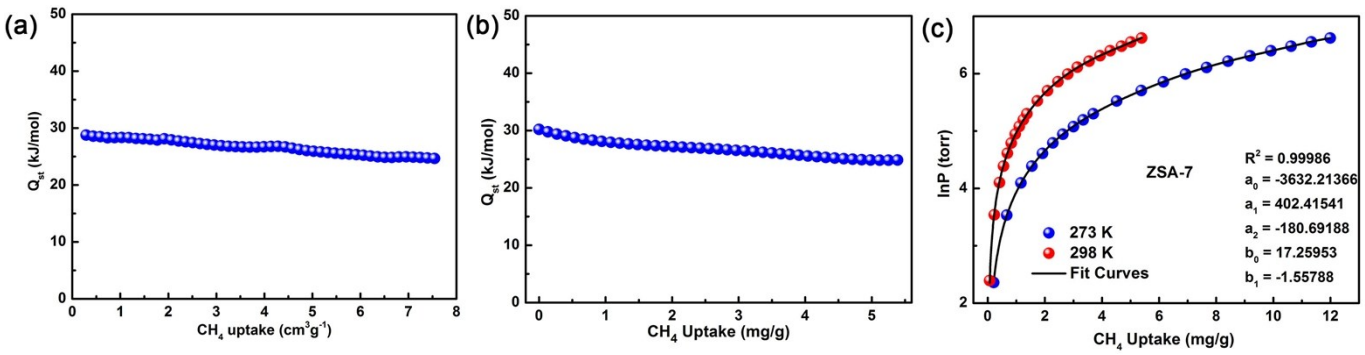

Fig. S19. Q_{st} of CH_4 for **ZSA-7**. (a) calculated by MicroActive soft; (b) calculated with virial method; (c) nonlinear curves fitting of CH_4.

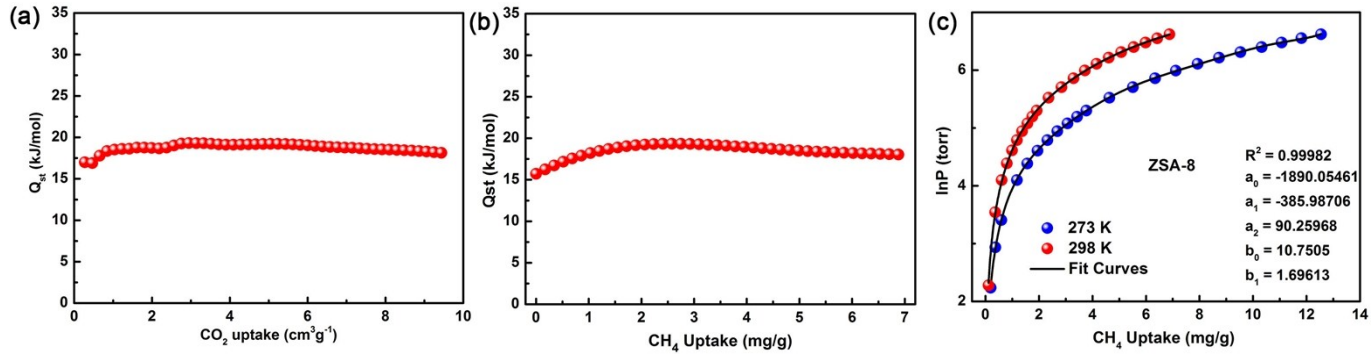

Fig. S20. Q_{st} of CH_4 for **ZSA-8**. (a) calculated by MicroActive soft; (b) calculated with virial method; (c) nonlinear curves fitting of CH_4.

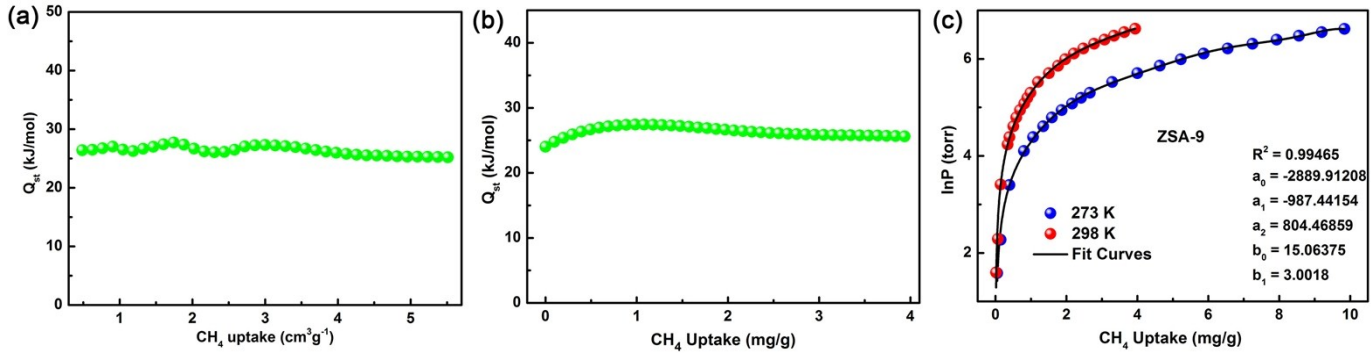

Fig. S21. Q_{st} of CH_4 for **ZSA-9**. (a) calculated by MicroActive soft; (b) calculated with virial method; (c) nonlinear curves fitting of CH_4.

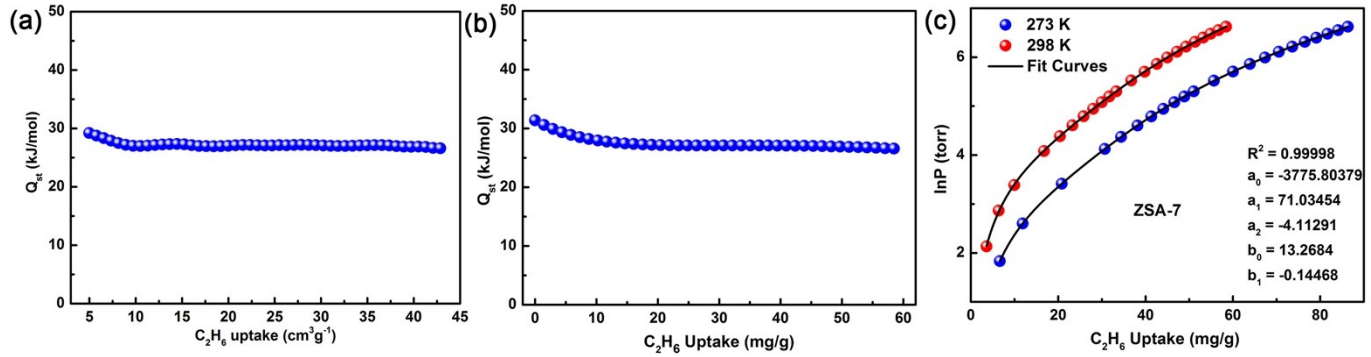

Fig. S22. Q_{st} of C_2H_6 for **ZSA-7**. (a) calculated by MicroActive soft; (b) calculated with virial method; (c) nonlinear curves fitting of C_2H_6.

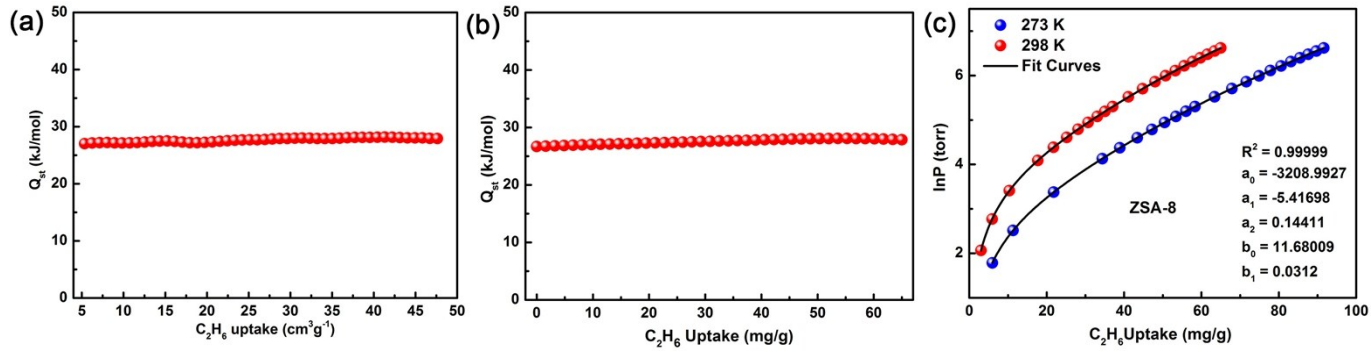

Fig. S23. Q_{st} of C_2H_6 for **ZSA-8**. (a) calculated by MicroActive soft; (b) calculated with virial method; (c) nonlinear curves fitting of C_2H_6.

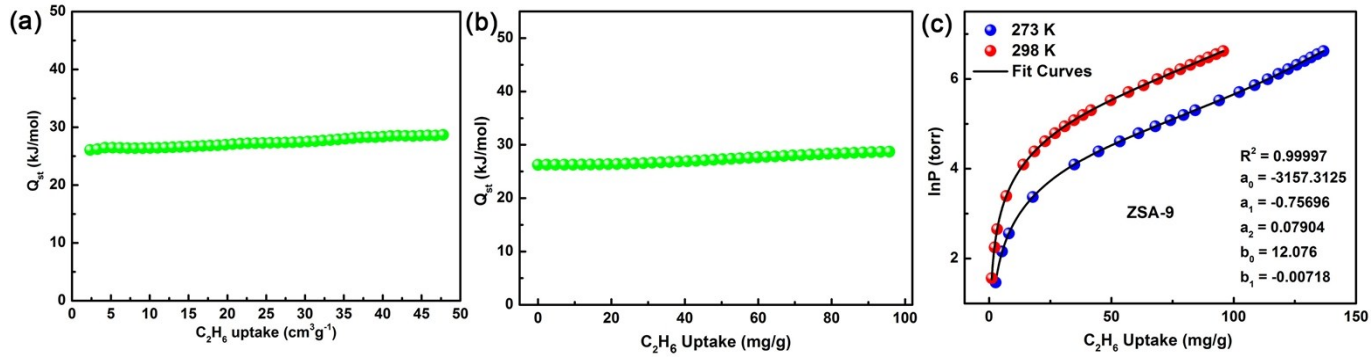

Fig. S24. Q_{st} of C_2H_6 for **ZSA-9**. (a) calculated by MicroActive soft; (b) calculated with virial method; (c) nonlinear curves fitting of C_2H_6.

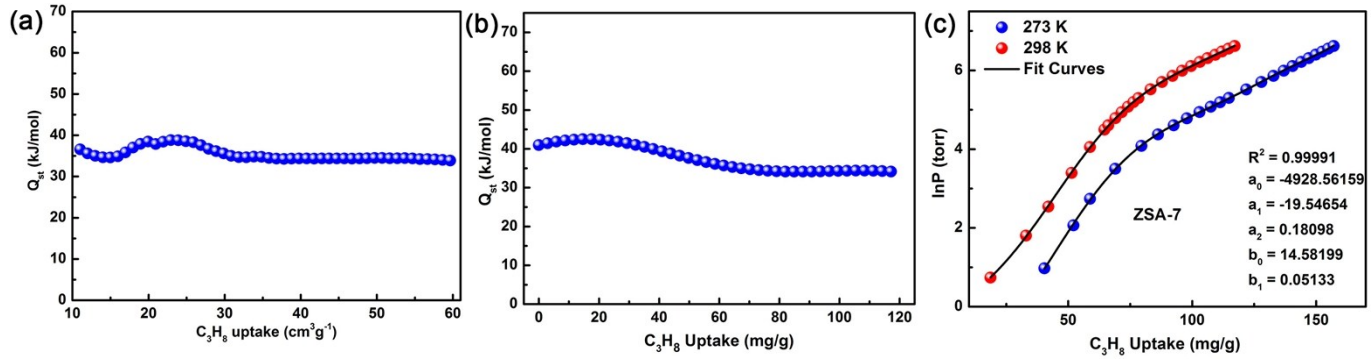

Fig. S25. Q_{st} of C_3H_8 for **ZSA-7**. (a) calculated by MicroActive soft; (b) calculated with virial method; (c) nonlinear curves fitting of C_3H_8.

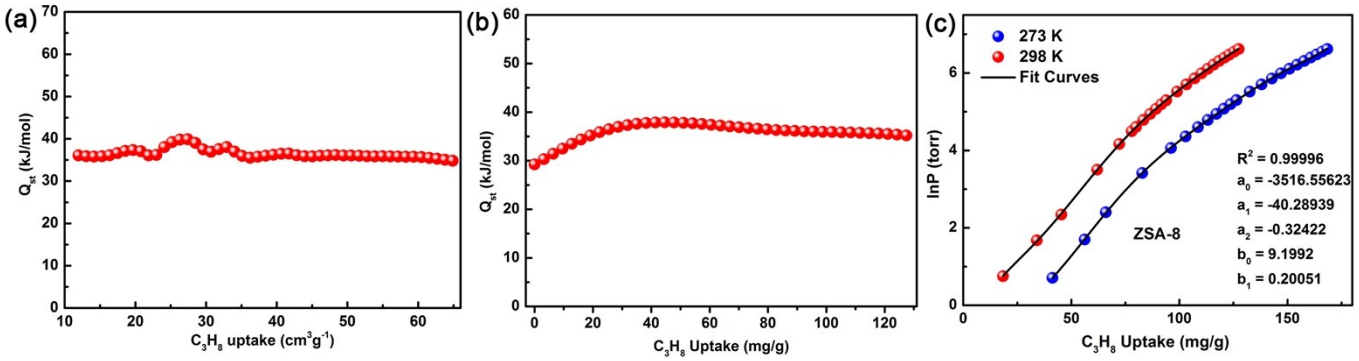

Fig. S26. Q_{st} of C_3H_8 for **ZSA-8**. (a) calculated by MicroActive soft; (b) calculated with virial method; (c) nonlinear curves fitting of C_3H_8.

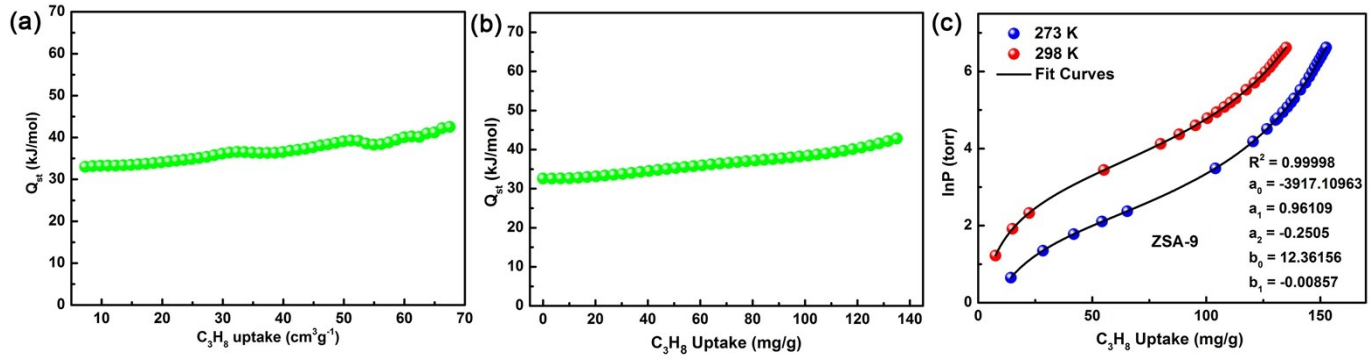

Fig. S27. Q_{st} of C_3H_8 for **ZSA-9**. (a) calculated by MicroActive soft; (b) calculated with virial method; (c) nonlinear curves fitting of C_3H_8.

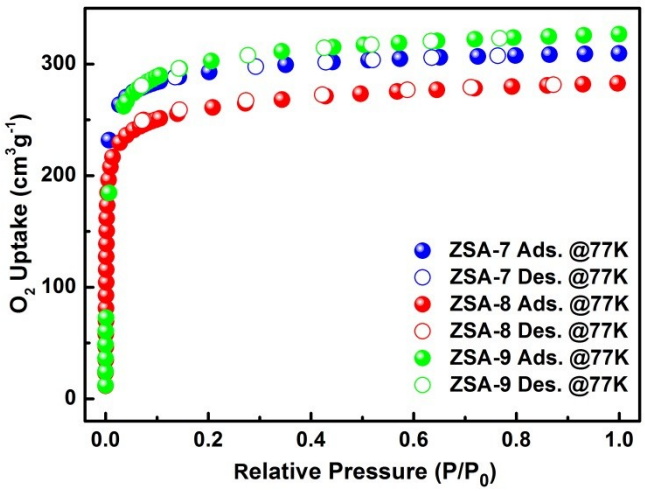

Fig. S28. O_2 sorption isotherms for **ZSA-7** (blue), **ZSA-8** (red) and **ZSA-9** (green) at 77 K.

S3. Supporting Tables

Table S1. Crystal data and structure refinements for **ZSA-7**, **ZSA-8** and **ZSA-9**.

Compound	**ZSA-7**	**ZSA-8**	**ZSA-9**
Formula	$C_{32}H_{64}Co_4N_{20}O_{24}$	$C_{36}H_{68}Co_4N_{16}O_{28}$	$C_{44}H_{86}Co_4N_{16}O_{25}$
Mw	1347.75	1408.78	1475.01
Temp (K)	296(2)	296(2)	296(2)
Wavelength (Å)	0.71073	0.71073	0.71073
Crystal system	Tetragonal	Tetragonal	Tetragonal
Space group	I4(1)/amd	I4(1)/amd	I4(1)/amd
a (Å)	19.1419(2)	18.125(8)	19.597(4)
b (Å)	19.1419(2)	18.125(8)	19.597(4)
c (Å)	21.8929(3)	22.375(11)	20.713(5)
V (Å^3)	8021.83(16)	7351(6)	7955(3)
Z, D_C (Mg/m^3)	4, 1.117	4, 1.273	4, 1.232
F(000)	2784	2912	3080
θ range (deg)	1.41 - 25.37	1.45 - 25.03	1.43 - 25.07
reflns collected/unique	14119 / 1920	22744 / 1740	24932 / 1884
R_{int}	0.0583	0.0493	0.0646
data/restraints/params	1920 / 18 / 113	1740 / 52 / 122	1884 / 68 / 138
GOF on F^2	1.049	1.132	1.059
R^1, wR^2 (I>2σ(I))	0.0730, 0.2192	0.0755, 0.2691	0.0667, 0.2156
R^1, wR^2 (all data)	0.1164, 0.2628	0.0957, 0.2999	0.0857, 0.2439

[a]$R_1 = \Sigma||F_o| - |F_c||/\Sigma|F_o|$, [b]$wR_2 = [\Sigma w(|F_o|^2 - |F_c|^2)/\Sigma|w(F_o^2)^2|^{1/2}$

Table S2. Selected bond lengths [Å] and angles [º] for **ZSA-7**.

ZSA-7			
Co(1)-O(1)	1.914(4)	N(1)#1-Co(1)-N(3)	91.40(17)
Co(1)-O(1)#1	1.914(4)	N(1)-Co(1)-N(3)	171.65(17)
Co(1)-N(1)#1	1.924(4)	O(1)-Co(1)-N(3)#1	92.17(17)
Co(1)-N(1)	1.924(4)	O(1)#1-Co(1)-N(3)#1	88.73(17)
Co(1)-N(3)	1.930(5)	N(1)#1-Co(1)-N(3)#1	171.65(18)
Co(1)-N(3)#1	1.930(5)	N(1)-Co(1)-N(3)#1	91.40(17)
O(1)-Co(1)-O(1)#1	178.8(2)	N(3)-Co(1)-N(3)#1	85.5(3)
O(1)-Co(1)-N(1)#1	95.54(15)	C(3)-O(1)-Co(1)	115.8(3)
O(1)#1-Co(1)-N(1)#1	83.62(15)	C(1)-N(1)-Co(1)	140.5(4)
O(1)-Co(1)-N(1)	83.62(15)	C(2)-N(1)-Co(1)	112.2(3)
O(1)#1-Co(1)-N(1)	95.54(15)	C(4')-N(3)-Co(1)	111.2(8)
N(1)#1-Co(1)-N(1)	92.6(2)	C(4)-N(3)-Co(1)	109.0(6)
O(1)-Co(1)-N(3)	88.73(17)	Co(1)-N(3)-H(3A)	109.9
O(1)#1-Co(1)-N(3)	92.17(17)	Co(1)-N(3)-H(3B)	109.9

Symmetry transformations used to generate equivalent atoms:
#1 -y+3/4,-x+3/4,-z+1/4 #2 -x,y,z #3 -x+1,y,z

Table S3. Selected bond lengths [Å] and angles [º] for **ZSA-8**.

ZSA-8			
Co(1)-O(1)#1	1.920(5)	N(1)#1-Co(1)-N(2)	91.55(19)
Co(1)-O(1)	1.920(5)	N(1)-Co(1)-N(2)	173.1(2)
Co(1)-N(1)#1	1.936(5)	O(1)#1-Co(1)-N(2)#1	89.6(2)
Co(1)-N(1)	1.936(5)	O(1)-Co(1)-N(2)#1	92.1(2)
Co(1)-N(2)	1.952(6)	N(1)#1-Co(1)-N(2)#1	173.1(2)
Co(1)-N(2)#1	1.952(6)	N(1)-Co(1)-N(2)#1	91.55(19)
O(1)#1-Co(1)-O(1)	177.7(3)	N(2)-Co(1)-N(2)#1	85.8(3)
O(1)#1-Co(1)-N(1)#1	84.16(17)	C(3)-O(1)-Co(1)	115.4(4)
O(1)-Co(1)-N(1)#1	94.21(18)	C(1)-N(1)-Co(1)	141.4(4)
O(1)#1-Co(1)-N(1)	94.21(18)	C(2)-N(1)-Co(1)	111.0(4)
O(1)-Co(1)-N(1)	84.16(17)	C(5)-N(2)-Co(1)	112.7(11)
N(1)#1-Co(1)-N(1)	91.8(3)	C(5')-N(2)-Co(1)	108.2(11)
O(1)#1-Co(1)-N(2)	92.1(2)		
O(1)-Co(1)-N(2)	89.6(2)		

Symmetry transformations used to generate equivalent atoms:
#1 -y+3/4,-x+3/4,-z+1/4 #2 x,-y+1/2,z

Table S4. Selected bond lengths [Å] and angles [º] for **ZSA-9**.

ZSA-9			
Co(1)-O(1)#1	1.898(4)	N(2)#1-Co(1)-N(1)	91.64(15)
Co(1)-O(1)	1.898(4)	N(2)-Co(1)-N(1)	170.82(16)
Co(1)-N(2)#1	1.933(4)	O(1)#1-Co(1)-N(1)#1	84.12(13)
Co(1)-N(2)	1.933(4)	O(1)-Co(1)-N(1)#1	98.03(14)
Co(1)-N(1)	1.944(4)	N(2)#1-Co(1)-N(1)#1	170.82(16)
Co(1)-N(1)#1	1.944(4)	N(2)-Co(1)-N(1)#1	91.64(15)
O(1)#1-Co(1)-O(1)	176.93(18)	N(1)-Co(1)-N(1)#1	92.0(2)
O(1)#1-Co(1)-N(2)#1	87.03(15)	C(3)-O(1)-Co(1)	116.4(3)
O(1)-Co(1)-N(2)#1	90.73(16)	C(1)-N(1)-Co(1)	142.5(3)
O(1)#1-Co(1)-N(2)	90.73(16)	C(2)-N(1)-Co(1)	110.0(3)
O(1)-Co(1)-N(2)	87.03(15)	C(7')-N(2)-Co(1)	111.3(13)
N(2)#1-Co(1)-N(2)	86.1(2)	C(7)-N(2)-Co(1)	107.0(13)
O(1)#1-Co(1)-N(1)	98.03(14)		
O(1)-Co(1)-N(1)	84.12(13)		

Symmetry transformations used to generate equivalent atoms:

#1 -y+3/4,-x+3/4,-z+1/4 #2 x,-y+3/2,z

Table S5. The refined parameters for the Dual-site Langmuir-Freundlich equations fit for the pure isotherms of CO_2, CH_4, C_2H_6 and C_3H_8 for **ZSA-7, ZSA-8, ZSA-9 and ZSA-1** at 298 K.

		q_{m1}	b_1	$1/n_1$	q_{m2}	b_2	$1/n_2$	R^2
ZSA-7	CO_2	1.62028	0.18442	1.0000	4.33212	0.01113	1.0000	0.99999
	CH_4	8.66643	2.04698E-4	1.1256	0.0185	0.06986	0.91254	0.99992
	C_2H_6	1.24389	0.07545	1.0265	5.35483	0.00193	0.9854	0.99997
	C_3H_8	3.01407	0.00785	1.0214	1.24853	1.71999	0.99407	0.99985
ZSA-8	CO_2	3.48942	0.06797	1.0506	3.60923	0.00407	0.96242	0.99999
	CH_4	158.10754	5.73758E-6	1.24945	0.25029	0.01698	0.89165	0.99996
	C_2H_6	1.12333	0.05765	1.09318	4.24679	0.00842	0.81987	0.99999
	C_3H_8	0.59315	2.83954	1.82462	6.66574	0.07638	0.41647	0.99998
ZSA-9	CO_2	0.79081	0.01741	1.27225	8.18131	5.18921E-4	1.24824	0.99985
	CH_4	0.00374	0.82379	1.13353	39.18373	3.5596E-5	1.10377	0.99937
	C_2H_6	0.02083	0.59471	1.02568	3.50526	0.00919	1.11512	0.99999
	C_3H_8	1.58099	0.09979	0.72514	1.90671	0.13894	1.31713	0.99999
ZSA-1	CO_2	1.89567	0.34431	0.9584	7.0931	0.00169	1.14831	0.99993
	CH_4	34.06727	9.27352E-5	1.06349	0.00318	0.11697	0.9856	0.99996
	C_2H_6	6.9836	0.00687	0.84171	1.41368	0.03719	1.10988	0.99999
	C_3H_8	4.29886	0.00939	1.14555	1.73448	0.93461	1.08672	0.99996